

Environmental CO₂ inhibits *Caenorhabditis elegans* egg-laying by modulating olfactory neurons and evokes widespread changes in neural activity

 Lorenz A. Fenk and Mario de Bono¹

Cell Biology Division, Medical Research Council Laboratory of Molecular Biology, Cambridge CB2 0QH, United Kingdom

Edited by Martin Chalfie, Columbia University, New York, NY, and approved May 22, 2015 (received for review December 11, 2014)

Carbon dioxide (CO₂) gradients are ubiquitous and provide animals with information about their environment, such as the potential presence of prey or predators. The nematode *Caenorhabditis elegans* avoids elevated CO₂, and previous work identified three neuron pairs called "BAG," "AFD," and "ASE" that respond to CO₂ stimuli. Using in vivo Ca²⁺ imaging and behavioral analysis, we show that *C. elegans* can detect CO₂ independently of these sensory pathways. Many of the *C. elegans* sensory neurons we examined, including the AWC olfactory neurons, the ASJ and ASK gustatory neurons, and the ASH and ADL nociceptors, respond to a rise in CO₂ with a rise in Ca²⁺. In contrast, glial sheath cells harboring the sensory endings of *C. elegans*' major chemosensory neurons exhibit strong and sustained decreases in Ca²⁺ in response to high CO₂. Some of these CO₂ responses appear to be cell intrinsic. Worms therefore may couple detection of CO₂ to that of other cues at the earliest stages of sensory processing. We show that *C. elegans* persistently suppresses oviposition at high CO₂. Hermaphrodite-specific neurons (HSNs), the executive neurons driving egg-laying, are tonically inhibited when CO₂ is elevated. CO₂ modulates the egg-laying system partly through the AWC olfactory neurons: High CO₂ tonically activates AWC by a cGMP-dependent mechanism, and AWC output inhibits the HSNs. Our work shows that CO₂ is a more complex sensory cue for *C. elegans* than previously thought, both in terms of behavior and neural circuitry.

neural circuit | behavioral choice | olfactory system | oviposition | glia

Most living matter creates temporal or spatial gradients of carbon dioxide (CO₂). Animals across phylogeny use such gradients to help detect food, conspecifics, or predators (1, 2). The ubiquity of CO₂ suggests that the ecologically relevant information it communicates will depend on the dynamics of the CO₂ stimulus and on context. CO₂-responsive excitable cells have been identified in mammals (3), arthropods (4), and nematodes (5, 6). However, the number of CO₂-responsive neurons that are functional in vivo, how they are embedded in neural circuits, and how they shape behavior is unclear.

CO₂ crosses membranes readily and dissolves to generate CO₂(aq), H⁺, and HCO₃⁻. Many proteins whose activity is modified by CO₂ or its solvation products have been identified. pH changes can modulate G protein-coupled receptors (7), Ca²⁺-activated K⁺ channels (8), inwardly rectifying K⁺ channels (9), two pore domain K⁺ channels (10), transient receptor potential (TRP) channels (11, 12), acid-sensing ion channels (ASICs) (13, 14), and Pyk2 and ErbB1/2 kinases (15). HCO₃⁻ modulates soluble adenylylase (16) and transmembrane guanylate cyclases (17); and CO₂(aq) has been proposed to regulate transmembrane guanylate cyclases (18) and connexin 26 (19) directly. Cells expressing any of these proteins potentially could transduce changes in CO₂/H⁺, raising the question: Do animals use a few specific sensory channels or a large distributed set to respond to ecologically meaningful fluctuations in CO₂? If there are many responsive neurons, how does each contribute to altered behavior or physiology?

In mammals, CO₂ levels are tightly controlled to ensure that blood pH remains stable. Peripheral sensors in the carotid bodies and incompletely defined central chemoreceptors respond to small changes in CO₂/H⁺ by homeostatically altering the breathing rate (3, 20). In concert, pH and HCO₃⁻ sensors in the kidneys regulate H⁺ and HCO₃⁻ excretion (21, 22). These mechanisms keep human blood pH close to 7.4, and in healthy individuals neurons experience only limited fluctuation in CO₂/H⁺. In contrast, in small invertebrates such as nematodes that breathe by diffusion through a gas-permeable skin and have limited buffering capacity, CO₂ levels in body fluid probably vary more widely, according to ambient CO₂ levels.

The nematode *Caenorhabditis elegans* avoids environments with elevated CO₂ (23, 24), and high CO₂ can adversely effect its development, mobility, fertility, and aging (25). Three neurons that respond robustly to CO₂ have been identified thus far in this animal: BAG neurons that also respond to O₂, the thermosensory AFD neurons, and the gustatory ASE neurons (5, 6). CO₂ responses in BAG neurons are mediated by a receptor-type guanylate cyclase, GCY-9, that signals via a cGMP-gated ion channel encoded by the *tax-2* and *tax-4* genes (6). The CO₂ responsiveness of AFD thermosensors is sculpted by previous acclimation temperature, suggesting experience-dependent cross-modulation between temperature- and CO₂-sensing mechanisms in this neuron (26). Acute changes in O₂ also alter *C. elegans*' CO₂ responsiveness: CO₂ avoidance is suppressed when O₂ approaches 21%, because of tonic signaling by the O₂-sensing neuron URX (26, 27).

Significance

Carbon dioxide (CO₂) gradients are ubiquitous, but fluctuations in CO₂ provide an important cue shaping animal behavior. This paradox suggests that CO₂ provides contextual information that is integrated with other inputs. Here, we show that *Caenorhabditis elegans* CO₂-sensing circuits are much more sophisticated than assumed hitherto. A surprisingly large number of neurons, including nociceptors, gustatory neurons, and olfactory neurons, respond to CO₂ in vivo. Glia also exhibit large Ca²⁺ responses to CO₂. Worms therefore may couple detection of CO₂ and other cues at the earliest stages of sensory processing. Besides avoiding CO₂, *C. elegans* stops laying eggs at high CO₂. Inhibition of oviposition involves sustained activation of the AWC olfactory neurons by CO₂ and enduring inhibition of neurons innervating the egg-laying muscles.

Author contributions: L.A.F. and M.d.B. designed research; L.A.F. performed research; L.A.F. and M.d.B. analyzed data; and L.A.F. and M.d.B. wrote the paper.

The authors declare no conflict of interest.

This article is a PNAS Direct Submission.

Freely available online through the PNAS open access option.

¹To whom correspondence should be addressed. Email: debono@mrc-lmb.cam.ac.uk.

This article contains supporting information online at www.pnas.org/lookup/suppl/doi:10.1073/pnas.1423808112/-DCSupplemental.

Here, we identify many additional *C. elegans* cells that respond to CO₂, including both neurons and glia. Some of these cells probably are intrinsically CO₂ sensitive. We show that elevated CO₂ inhibits egg-laying, and tonically represses the hermaphrodite-specific neurons (HSNs) critical for normal egg-laying behavior. CO₂ inhibition of egg-laying involves the AWC olfactory neurons, which are persistently stimulated at high CO₂ by a cGMP-dependent mechanism.

Results

Several CO₂-Evoked Responses Do Not Require Previously Identified CO₂ Sensors. Only one chemosensory transducer of CO₂ has been identified in *C. elegans*, GCY-9, which is required for CO₂ sensitivity in BAG neurons (6). The inherent complexity of CO₂ as a stimulus and the numerous molecules whose activity is sensitive to CO₂/H⁺ in vitro (3) led us to conjecture that *C. elegans* has undiscovered CO₂-sensing neurons and pathways. To investigate this possibility, we examined CO₂-evoked locomotory responses in *gcy-9* mutants and in BAG-ablated animals, a kind gift of Manuel Zimmer, Institute of Molecular Pathology, Vienna. We placed animals on a thin bacterial lawn in a microfluidic chamber and exposed them to a 0–5–0% CO₂ stimulus train (Fig. 1). Animals from the N2 laboratory reference strain responded to rising CO₂ by freezing briefly, turning sharply (these turns are called “omega turns” because of their shape), and resuming forward movement with an altered course at a higher speed (Fig. 1A). Faster movement was maintained while CO₂ was high (Fig. 1A) (5). When CO₂ dropped from 5 to 0%, N2 animals transiently sped up before gradually settling (Fig.

1A). BAG-ablated animals and *gcy-9* mutants showed little turning during the 0–5% rise in CO₂ and failed to speed up transiently as CO₂ dropped from 5 to 0%. However, other features of the N2 locomotory response were not reduced significantly (Fig. 1A and B). Thus, *gcy-9* and BAG neurons contribute part but not all of *C. elegans*’ acute locomotory response to CO₂.

A cGMP-gated ion channel subunit encoded by *tax-4* sustains CO₂ responses not only in BAG neurons but also in AFD and probably in ASE neurons (5). Like *gcy-9* mutants and BAG-ablated animals, *tax-4(p678null)* mutants showed severe defects in turning following a 0–5% rise in CO₂ (Fig. 1C), as would be expected if BAG was defective. However, other features of the locomotory response to CO₂ were unaffected or even enhanced. Most prominently, *tax-4* mutants increased their speed more strongly than N2 controls at 5% CO₂ (Fig. 1C). This heightened locomotory arousal suggests the existence of parallel pathways that inhibit and promote rapid movement at high CO₂, whose function is impaired and intact, respectively, in *tax-4* mutants.

BAG neurons are activated not only by a rise in CO₂ but also by a decrease in O₂ (28). A set of elegant experiments has shown that activating BAG by reducing O₂ or using channelrhodopsin inhibits *C. elegans* movement (28). We speculated that tonically elevated BAG signaling at 5% CO₂ inhibits locomotion and that the transient increase in movement when CO₂ levels drop reflects disinhibition of the forward locomotion circuit resulting from a decrease in BAG activity. This scenario would explain both why *tax-4* mutants move faster than N2 worms at high CO₂ (Fig. 1C) and why *gcy-9* mutants and BAG-ablated animals lack the CO₂ OFF response (Fig. 1A and B). To test the model, we expressed

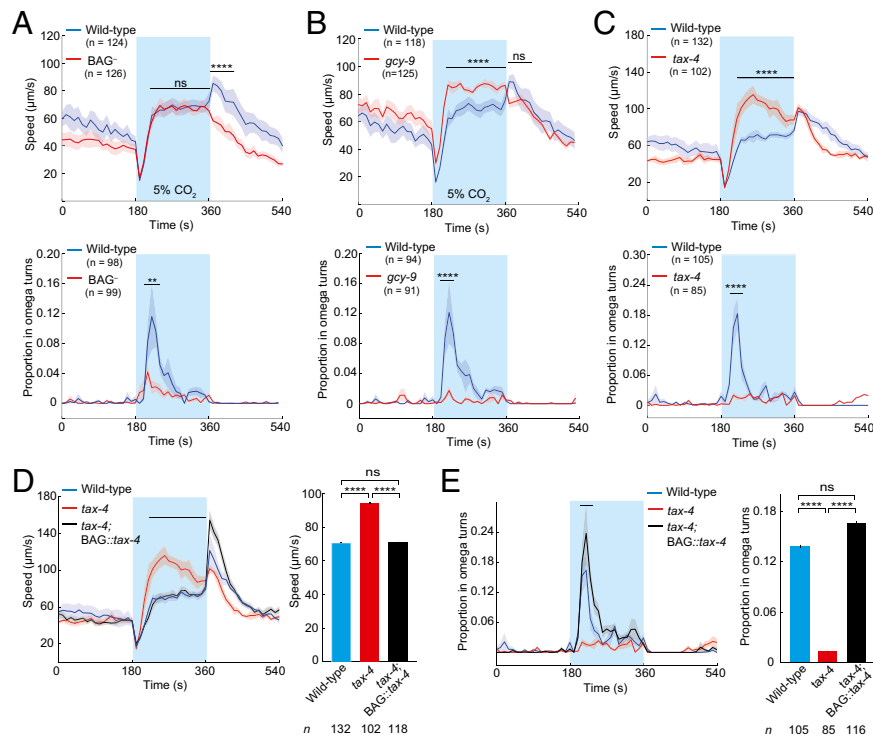


Fig. 1. A subset of CO₂-evoked changes in behavior is retained in *gcy-9* and *tax-4* mutants. (A–C) CO₂-evoked changes in speed (Upper) and omega turns (Lower) in N2 (wild-type) and BAG-ablated (BAG⁻) (A), *gcy-9(n4470)* (*gcy-9*) (B), and *tax-4(p678)* (*tax-4*) (C) animals. Solid lines indicate the mean, and the shaded areas indicate the SEM. ****P < 0.0001; **P < 0.01; ns, not significant; Mann-Whitney *u* test. In this and all subsequent figures, black bars indicate time intervals used for statistical comparison; blue shading indicates stimulation with CO₂. Speed and omega turns were analyzed in the same set of worms. However, the exact number of animals present in the region analyzed fluctuates over time as animals leave or re-enter the food lawn. *n* refers to the number of animals in the time windows used for statistical comparisons, which differ for speed and omega turns. (D and E) Selectively expressing *tax-4* in BAG neurons using a *flp-17p::tax-4* cDNA transgene rescues the speed (D) and omega turn (E) defects of *tax-4(p678)* mutants exposed to 5% CO₂. The background O₂ level in this and subsequent experiments is 21%.

tax-4 cDNA selectively in BAG using the *flp-17* promoter (29). This transgene restored CO₂-evoked omega turns (Fig. 1D) and wild-type locomotory activity at 5% CO₂ to *tax-4* mutants (Fig. 1E). It also conferred a larger speed OFF response than observed in N2 animals, perhaps because of overexpression of *tax-4* (Fig. 1E). Thus, BAG neurons promote CO₂ avoidance by stimulating turning when CO₂ rises and also slow down dispersal from high CO₂ by inhibiting rapid movement at high CO₂. Moreover, the striking locomotory response of *tax-4* mutants to CO₂ implies that there are unidentified CO₂ sensors in *C. elegans*.

Many *C. elegans* Sensory Neurons Respond to CO₂. Our behavioral data prompted us to seek other CO₂-responsive neurons by using in vivo Ca²⁺ imaging of neurons expressing the ratiometric sensor YC3.60. We detected robust CO₂-evoked Ca²⁺ increases in the nociceptive ADL and ASH neurons, the food/pheromone-sensing ASK neurons, the AWC olfactory neurons, and the ASJ photoreceptors/pheromone sensors (Fig. 2A). As a notable exception, YC3.60 reported that the ASG gustatory neurons were not activated but were slightly inhibited by CO₂. The majority of the CO₂-responsive neurons we identified exhibited a Ca²⁺ transient followed by a tonic component that decayed partially or completely within the 3-min window of stimulation. Interestingly, CO₂ responses in the AWC neurons deviated from this pattern: The relatively slow Ca²⁺ rise showed no sign of decay over our 3-min recording, reminiscent of the CO₂ response reported in the ASE gustatory neurons (5).

These imaging results were unexpected, especially because previous studies failed to detect CO₂-evoked Ca²⁺ responses in the nociceptive ADL (6) and ASH neurons (5, 6). Such discrepancies may reflect differences in stimulus regimes, imaging conditions, Ca²⁺ indicators, or transgenic lines used. In the case of ASH, the differences between our results here and in a previous study (5) appear to be associated with the transgenic imaging lines used.

A potential confound in using cameleon or GCaMP sensors to measure CO₂-evoked responses is the pH sensitivity of fluorophores (30). Acidification caused by a rise in CO₂ could alter the fluorescence signal from Ca²⁺ sensors independently of changes in Ca²⁺. In vitro, the fluorescence of YC3.60 fluorophores is pH resistant (31). Nevertheless, to control for this possibility in vivo, we generated a Ca²⁺-insensitive derivative of YC3.60 by mutating its Ca²⁺-binding sites (Methods and Fig. S1), expressed the probe in the AWC, ASJ, and ADL neurons, and imaged CO₂ responses. In none of these cells did we observe a CO₂-evoked increase in the YFP/CFP fluorescence ratio, contrasting with our results using wild-type YC3.60 (Fig. S1). Our data suggest that ADL, ASH, ASJ, ASK, and AWC sensory neurons are all CO₂ responsive.

How is complexity at the sensory level represented in downstream interneurons? Many of the CO₂-responsive neurons we have identified, including ASE, ASH, ASK, ADL, and AWC, make synaptic connection onto the AIA interneurons. Previous studies suggest AWC, ASH, and ASK inhibit AIA (32, 33)

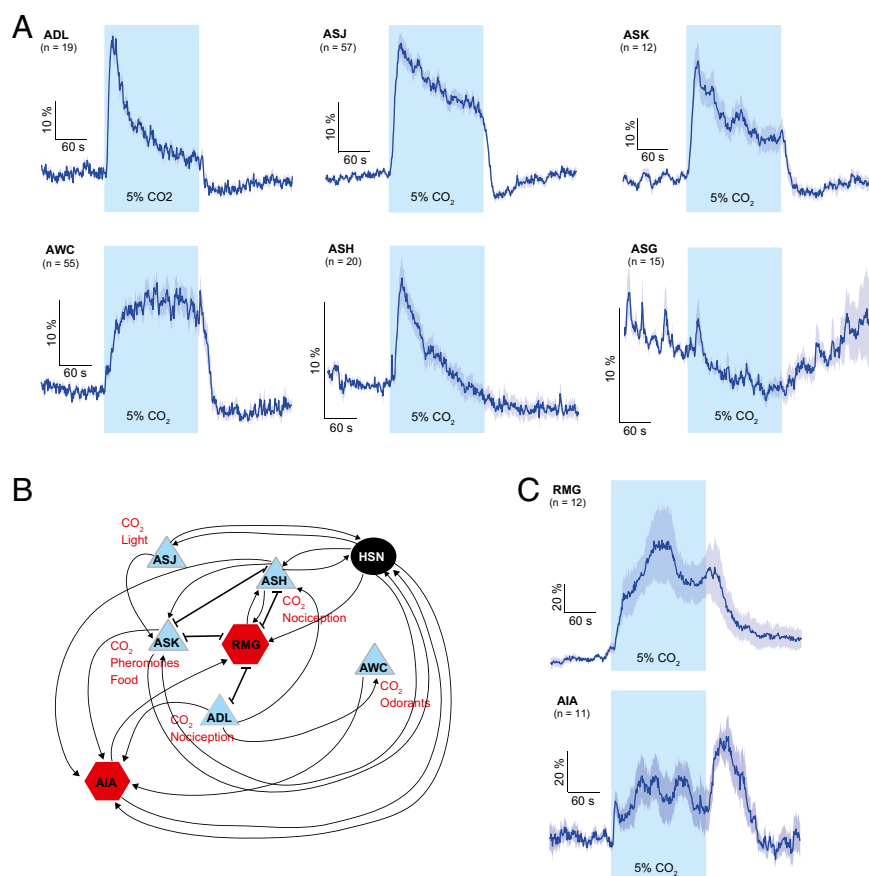


Fig. 2. Many *C. elegans* neurons show CO₂-evoked Ca²⁺ responses. (A) Averaged Ca²⁺ responses of sensory neurons to a 5% CO₂ stimulus measured using YC3.60. Each blue trace represents the average percentage change in R/R_0 for the indicated neuron, where R is the fluorescence emission ratio at a given time point and R_0 is its initial value. The shaded region indicates the SEM of the mean response. (B) Circuit diagram showing connections between newly identified CO₂-responsive neurons and two major downstream interneurons, AIA and RMG. (C) CO₂-evoked Ca²⁺ responses in RMG and AIA interneurons. Individual traces are plotted in Fig. S2.

whereas ASEL inputs probably are excitatory (34). A rise in CO₂ evoked a rise in AIA Ca²⁺, consistent with excitatory input (Fig. 2C and Fig. S24). Removal of the CO₂ stimulus, however, evoked a transient further rise in Ca²⁺, which is explained most easily as a disinhibitory response, before Ca²⁺ returned to baseline (Fig. 2C and Fig. S24). These data suggest that CO₂ responses in AIA interneurons reflect compound excitatory and inhibitory inputs, although we have not attempted to map how individual sensory neurons contribute to the CO₂-evoked Ca²⁺ responses in AIA.

CO₂ Evokes a Persistent Ca²⁺ Drop in Glial Sheath Cells of Amphid and Phasmid Neurons. In mammals astrocytes in the retrotrapezoid nucleus respond to CO₂/H⁺ and probably contribute to respiratory drive when CO₂ levels increase by releasing ATP (35, 36). Astrocytes are glia and can have multiple functions, including provision of nutrients, maintenance of extracellular ion balance, and in some cases release of neurotransmitters. *C. elegans* also has glia, including sheath cells that envelop the sensory endings of chemosensory and mechanosensory neurons (37, 38). For example, the ciliated sensory endings of neurons in the major chemosensory organs of the worm, the amphids and phasmids, traverse the amphid or phasmid sheath cells in narrow membranous tubes and enter the sensillar channel within the sheath cell.

Using the YC3.60 Ca²⁺ reporter, we examined if the amphid or phasmid sheath cells respond to changes in CO₂. Both sheath cell types exhibited large and long-lasting decreases in Ca²⁺ at high CO₂, with slow ON and OFF kinetics (Fig. 3A and B). The changes in YFP and CFP fluorescence were anticorrelated, as would be expected if they reflect FRET (Fig. 3C). The unusually high YFP/CFP ratio of sheath cells at 0% CO₂, even compared with stimulated ON neurons (Fig. S34), suggests that these glial cells have high cytoplasmic Ca²⁺ under our imaging conditions. The sharp and sustained decrease in sheath cell Ca²⁺ evoked by high CO₂ suggests closure of Ca²⁺ channels by hyperpolarization and/or increased activity of Ca²⁺ pumps in these cells.

Previous work has shown that an ASIC channel, ACD-1, functions in amphid sheath cells to promote acid avoidance and chemotaxis to lysine (39). Whether disrupting *acd-1* or changing pH alters Ca²⁺ levels in amphid sheath cells has not been investigated. However, studies of *acd-1* heterologously expressed in *Xenopus* oocytes suggest it encodes a constitutively open Na⁺-permeable channel that, unusually for an ASIC, is inhibited by protons. These data raised the possibility that sheath cell hyperpolarization at high CO₂ is caused by H⁺-induced closure of ACD-1 channels. However, the CO₂-evoked Ca²⁺ response in amphid sheath cells was not altered substantially in *acd-1(bz90)* deletion mutants (Fig. S3B). Thus, other mechanisms must underlie this response.

AWC and ASJ Neurons May Be Primary CO₂ Sensors. Are any of the CO₂-responsive cells we have identified endogenously CO₂ sensitive, or do they respond to inputs from presynaptic CO₂ sensors? The intrinsic CO₂ chemosensitivity of BAG neurons has been established by showing that their CO₂-evoked Ca²⁺ responses are not reduced in mutants defective in synaptic transmission (5, 6) and has been demonstrated most elegantly by showing that GCY-9, a receptor guanylyl cyclase required for BAG neurons to respond to CO₂, can confer CO₂ responsiveness on a heterologous neuron (6). AFD and ASE neurons also may be primary CO₂ sensors: Their responses are not diminished in synaptic transmission mutants (5), although for AFD, which has gap junctions with AIB, we cannot exclude the possibility that gap junctions transmit CO₂ responses from presynaptic neurons. With this caveat, imaging CO₂-evoked responses in mutants defective in chemical neurotransmission can provide valuable information about the origin of the neural responses (e.g., refs. 5, 40, and 41). The AWC and ASJ neurons are thought to lack gap junctions (42), rendering direct electrical input unlikely. Both pairs of neurons responded robustly to CO₂ in *unc-13* mutants, which are defective in synaptic vesicle release (43), and in mutants of the CAPS (Ca²⁺-dependent activator protein for secretion) ortholog *unc-31*, which are defective in release of dense-core vesicles (Fig. 4A–D) (44). A mutation in *unc-64* syntaxin, which simultaneously disrupts both synaptic and dense core vesicle release, also did not diminish CO₂ responses in AWC neurons (Fig. 4A). These data support the notion that AWC is endogenously CO₂ sensitive. For the ASJ neurons, disrupting *unc-64* reduced CO₂-evoked Ca²⁺ responses to about 60% of the wild-type value (Fig. 4D). Retention of the response is consistent with ASJ being intrinsically CO₂ sensitive, but the reduced size of the response indicates that synaptic and/or neuropeptidergic input increases the response magnitude. Although these results are consistent with AWC and ASJ neurons being primary sensors for CO₂ and/or its metabolites, proving this hypothesis requires the identification of a molecular CO₂ sensor in these neurons.

CO₂-evoked responses in ASH and ASK neurons also appear not to require chemical input (Fig. S4). However, because gap junctions connect ASH and ASK neurons not only to each other but also to numerous synaptic partners, intrinsic CO₂ sensitivity cannot be inferred. One of these partners, the RMG inter/motor neuron (42), makes gap junctions to ASH, ASK, and ADL CO₂-responsive neurons (Fig. 2B) (42, 45). RMG Ca²⁺ increased in response to 5% CO₂ (Fig. 2C and Fig. S2B), although the responses were less stereotyped across individuals than those of the sensory neurons. We have not attempted to relate RMG Ca²⁺ responses to specific sensory neuron input.

cGMP channel subunits encoded by the *tax-4* and *tax-2* genes are expressed in four of the CO₂-responsive neurons we have identified here: ASJ, ASK, AWC, and ASG. The previously studied sensory responses mediated by these neurons [e.g., ASJ

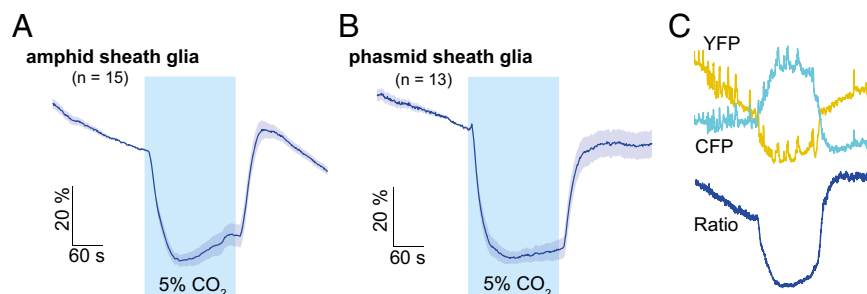


Fig. 3. Amphid and phasmid glial sheath cells are hyperpolarized by high CO₂. (A and B) Amphid (A) and phasmid (B) sheath glia exhibit a large, sustained decrease in Ca²⁺ when CO₂ levels rise. (C) Antagonistic changes in YFP and CFP fluorescence in phasmid sheath cells, confirming FRET.

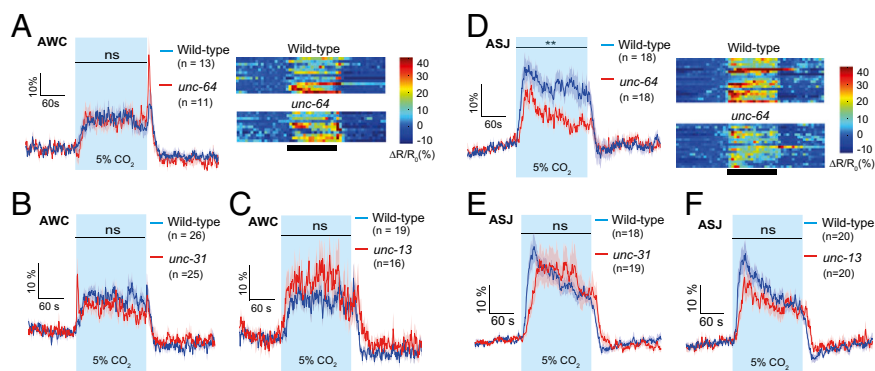


Fig. 4. Mean Ca^{2+} responses evoked by 5% CO_2 in AWC olfactory neurons (A–C) or ASJ chemosensory neurons (D–F) compared between wild-type (blue traces) and *unc-64*(e246) (A and D), *unc-31*(e928) (B and E), and *unc-13*(e51) (C and F) mutants (red traces). *unc-31* and *unc-13* animals are defective in the release of dense-core and synaptic vesicles, respectively; *unc-64* mutants are defective in both. Heat maps of the individual traces are included for A and D. ns, not significant; ** $P < 0.01$; Mann–Whitney u test. n = number of neurons imaged.

responses to light (46); ASK responses to pheromones and food (45, 47); and AWC responses to odors (48, 49)] are disrupted in *tax-2* or *tax-4* mutants. Do CO_2 responses in these neurons also depend on these cGMP channels? To examine this possibility, we imaged CO_2 -evoked responses in ASJ, AWC, and ASK neurons in a *tax-4*(p678)-null mutant background. *tax-4* mutants retained robust CO_2 responses in ASJ and ASK neurons (Fig. 5A and B), although, interestingly, loss of *tax-4* prevented Ca^{2+} levels in ASJ from returning promptly to baseline when the CO_2 stimulus was removed. In contrast, CO_2 -evoked responses in AWC neurons were greatly diminished in *tax-4* mutants (Fig. 5C). Selective expression of *tax-4* cDNA in AWC using a *ceh-36* promoter fragment (50) was sufficient to restore Ca^{2+} responses in *tax-4* mutants to wild-type levels (Fig. 5C and D). These data suggest that CO_2 sensing in AWC neurons, as in BAG neurons (5, 6), involves cGMP signaling.

The *tax-4*-independent, sustained Ca^{2+} responses of ASJ and ASK make them candidates to mediate the persistent increase in speed evoked by 5% CO_2 (Fig. 1A–D). To test this possibility, we ablated ASJ or ASK and measured locomotory activity. However, neither disruption prevented animals from modulating their speed in response to changing CO_2 (Fig. S5).

C. elegans Suppress Egg-Laying in High CO_2 . How do the CO_2 -evoked neural responses we have identified contribute to *C. elegans* behavior? Studies of CO_2 -evoked responses have focused primarily on locomotion, either in spatial or temporal CO_2 gradients (5, 6, 23, 24). As an alternative paradigm, we examined whether CO_2 altered egg-laying behavior. We hypothesized that mechanisms should have evolved to prevent worms from exposing their offspring to adverse concentrations of CO_2 (25, 51). To test this idea, we placed individual worms on thin bacterial lawns, exposed them to either 5% or atmospheric CO_2 concentrations, and compared the number of eggs laid by each group after 2 h. Strikingly, N2 animals essentially stopped laying eggs at 5% CO_2 , implying that CO_2 has an immediate and long-lasting inhibitory effect on egg-laying (Fig. 6A and B). Because N2 worms have experienced a long period of domestication in the laboratory, we also studied the effects of CO_2 on egg-laying in the Hawaiian wild strain CB4856. Like N2 worms, these animals stopped laying eggs in high CO_2 (Fig. S6A).

BAG neurons are a major source of FLP-17 (FMRFamide-like peptide) peptides, which, together with FLP-10 peptides, are ligands of the G protein-coupled receptor EGL-6 (egg-laying defective) (29). Activating mutations in EGL-6 inhibit egg-laying and the HSN egg-laying motor neurons, making BAG neurons plausible candidates to mediate the inhibitory effect of CO_2 . However, disrupting *gcy-9* (Fig. 6C) or ablating BAG (Fig. S6B)

did not reduce the inhibitory effect of CO_2 on egg-laying. The *tax-2*(p694) promoter mutation, which disrupts CO_2 responsiveness in the BAG, AFD, and ASE sensory neurons, also did not diminish

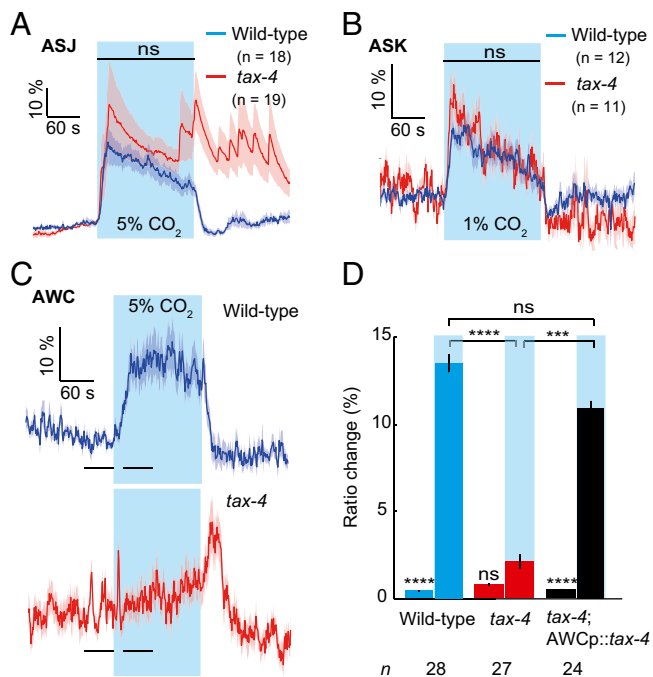


Fig. 5. TAX-4 is required cell autonomously for AWC CO_2 responses. (A and B) The cGMP-gated channel subunit TAX-4 is not required for ASJ (A) or ASK (B) CO_2 responses. Shown are average responses of *tax-4*(p678) mutants (red traces) and wild-type animals (blue traces). Note that 1% CO_2 was used to stimulate ASK. (C) Mean Ca^{2+} responses to 3-min stimulation with 5% CO_2 of wild-type (blue; Top), *tax-4*(p678) mutants (red; Middle), and *tax-4*(p678) animals expressing a *pceh-36::tax-4* cDNA transgene selectively in AWC (black; Bottom). (D) Quantification of data shown in C. Shaded areas indicate CO_2 stimulus; error bars indicate SEM. For comparisons across time intervals shown in C, **** $P < 0.0001$, *** $P < 0.001$; ns, not significant; Mann–Whitney u test.

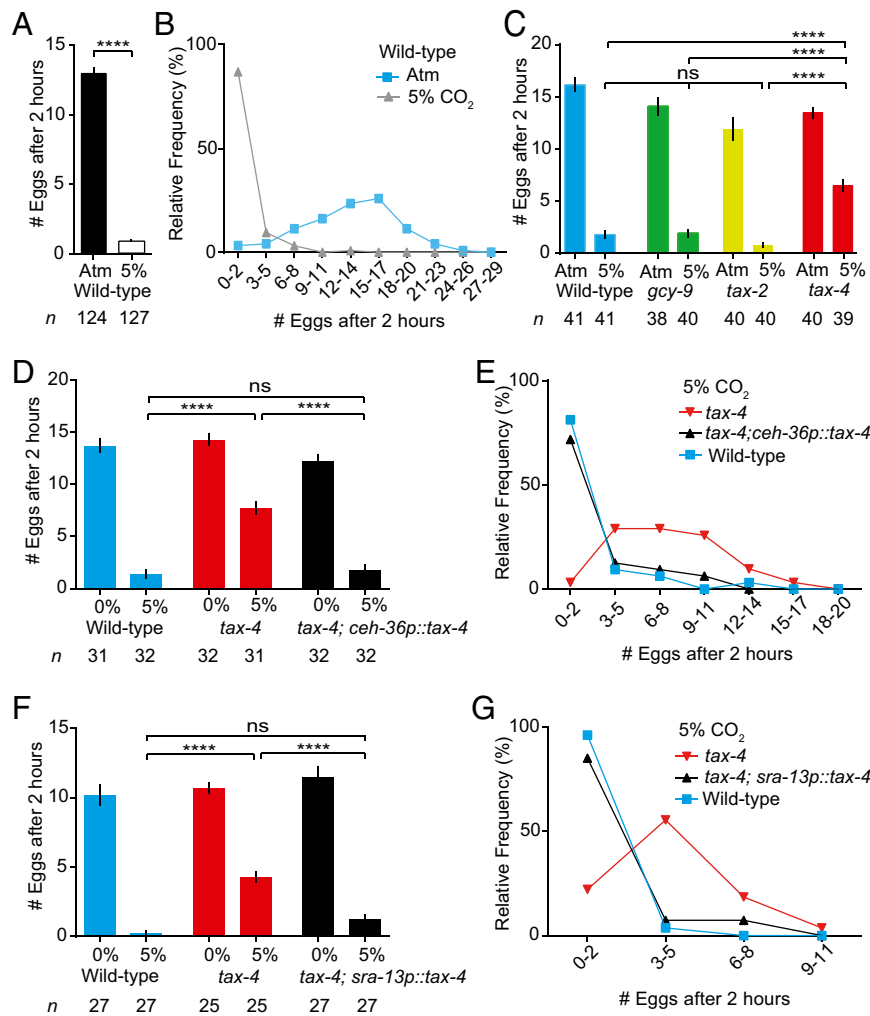


Fig. 6. CO₂ inhibition of egg-laying involves the AWC olfactory neurons. (A) Number of eggs laid per N2 hermaphrodite (wild-type) over 2 h by animals kept at atmospheric CO₂ (Atm) or 5% CO₂, plotted as mean ± SEM; *****P* < 0.0001; Kolmogorov–Smirnov test. (B) Distribution of egg-laying frequencies; data are from A. (C) Number of eggs laid by the genotypes indicated. At 5% CO₂ *gcy-9*(*n*4470) mutants and animals bearing a *tax-2*(*p*694) promoter mutation behave similarly to N2 reference wild-type animals. A *tax-4*-null mutation, *tax-4*(*p*678), significantly reduces the inhibitory effect of CO₂ compared with all other genotypes. Data are shown as mean ± SEM; *****P* < 0.0001; ns, not significant; Kruskal–Wallis ANOVA with Dunn’s multiple comparisons test. (D–G) Expressing *tax-4* cDNA in AWC olfactory neurons using either a cell-specific *ceh-36* promoter fragment (D and E) or the *sra-13* promoter (F and G) fully rescues the *tax-4* mutant phenotype. *****P* < 0.0001; ns, not significant; Kruskal–Wallis ANOVA with Dunn’s multiple comparisons test. E and G plot the distribution of egg-laying frequencies using the data from D and F, respectively.

CO₂’s effect on egg-laying (Fig. 6C) (5, 6). In contrast, the putative null alleles *tax-4*(*p*678) or *tax-2*(*p*671) significantly attenuated the inhibitory effect of CO₂ on egg-laying (Fig. 6C and Fig. S6C). These data suggest that one or more neurons functionally impaired in *tax-4*(*p*678) and *tax-2*(*p*671) mutants but spared in *tax-2*(*p*694) promoter mutants inhibit(s) egg-laying at 5% CO₂, leaving the ASG, ASI, ASJ, ASK, AWB, and AWC neurons as possible candidates (5, 48, 52). Expressing *tax-4* cDNA under the control of the *sra-13* promoter, whose expression pattern overlaps with that of *tax-4* only in AWC neurons (53), or under an apparently AWC-specific *ceh-36* promoter fragment (50) fully rescued the egg-laying phenotype of *tax-4* mutants (Fig. 6C), just as it rescued the defects in AWC Ca²⁺ response (Fig. 6 D–G). These data suggest that sustained stimulation of AWC neurons by elevated CO₂ can inhibit egg-laying.

Given the *egl-6*(*gf*) data referred to previously (29), we speculated that, although BAG neurons are not necessary for CO₂ to inhibit egg-laying, they might contribute as part of a redundant array of CO₂ sensors. To test this hypothesis, we expressed *tax-4* cDNA selectively in BAG neurons of *tax-4*(*p*678) mutants using

the *flp-17* promoter and examined CO₂-induced inhibition of egg-laying (Fig. S6D). We observed a weak but significant rescue of egg-laying inhibition. BAG neurons therefore may play a minor role in inhibiting egg-laying at high CO₂, although we cannot rule out the possibility that the small effect reflects leaky expression in AWC from the *pflp-17::tax-4* transgene.

CO₂ Tonically Inhibits HSNs. The HSNs are critical regulators of egg-laying and link the egg-laying circuit to the rest of nervous system (54). Ca²⁺ spikes in HSNs correlate with and likely trigger egg-laying events (55), because optogenetic stimulation of HSNs is sufficient to drive egg-laying (56–58). Does inhibition of egg-laying by elevated CO₂ involve inhibition of HSN motor neurons? To test this notion, we imaged Ca²⁺ in HSNs while raising CO₂ concentrations from 0 to 5%. HSNs are unusual in *C. elegans* because they spontaneously generate trains of Ca²⁺ transients (Fig. 7A). Upon addition of CO₂ we observed a decrease in HSN Ca²⁺ spikes that was both immediate and persistent. We also saw a general decrease in Ca²⁺ levels (Fig. 7A). Removal of CO₂ frequently was followed by a burst of Ca²⁺ transients in

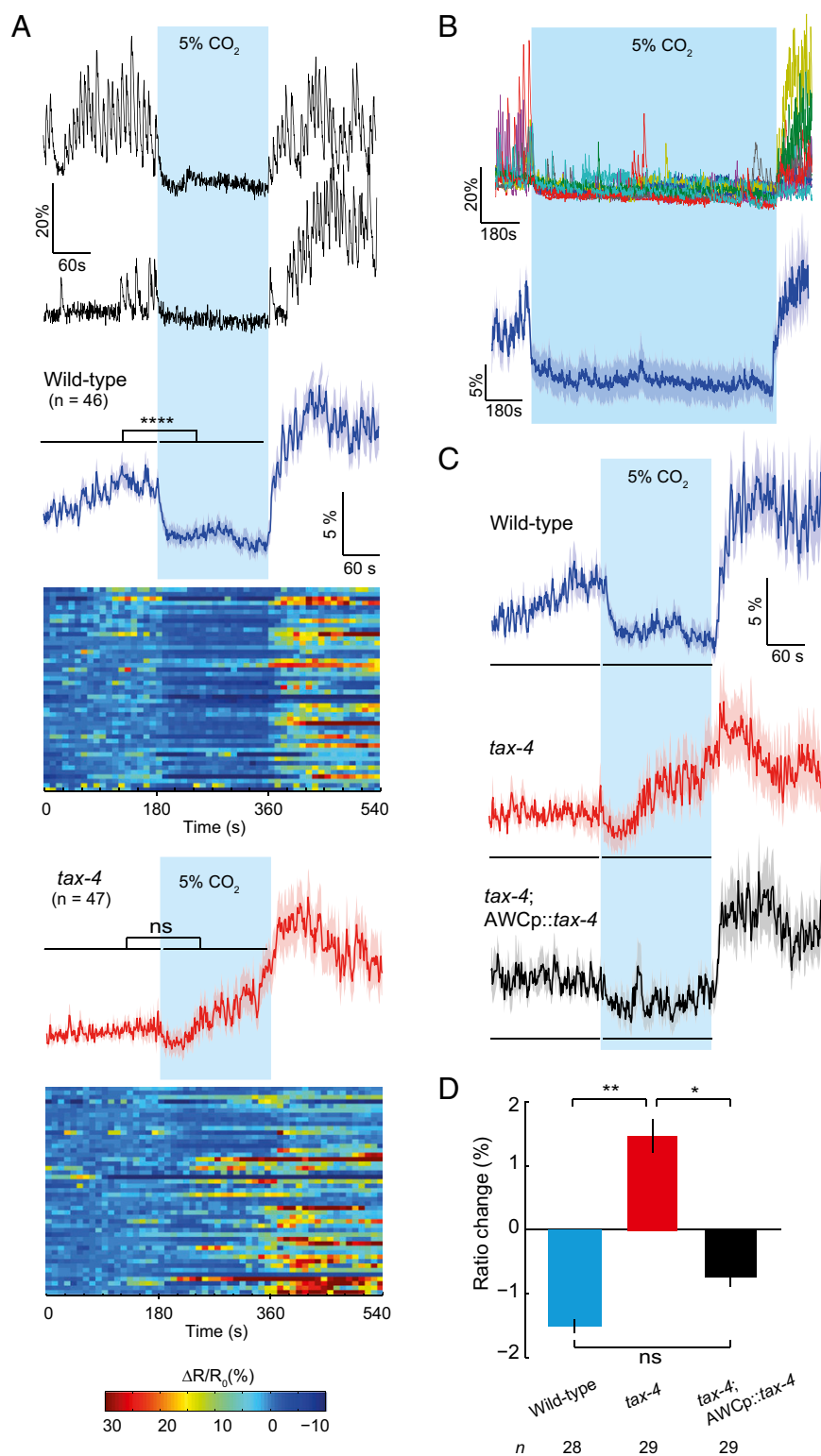


Fig. 7. HSNs are tonically inhibited by CO₂. (A) HSN Ca²⁺ transients are suppressed at high CO₂ in wild-type N2 (Upper) but not in *tax-4*(*p678*) mutants (Lower). The 5% CO₂ stimulus used is highlighted in blue. Shown are two sample traces, the average HSN response, and a color-coded pile-up of each response. *****P* < 0.0001; Mann–Whitney *u* test; ns, not significant. Shown are the average HSN response and a pile-up of heat maps for each response. All responses are aligned to the stimulus train. (B) Inhibition of HSNs by elevated CO₂ persists for at least 20 min. Shown are 11 individual traces overlaid on each other (Upper) and the average response (Lower). (C and D) The *tax-4*(*p678*) Ca²⁺ imaging phenotype in HSN can be rescued by expressing *tax-4* cDNA in the AWC olfactory neurons. ***P* < 0.01; **P* < 0.05; ns, not significant; Mann–Whitney *u* test.

HSNs, suggesting poststimulation rebound (Fig. 7A). The effects of CO₂ on HSNs, like CO₂'s effects on egg-laying and AWC Ca²⁺

responses, were persistent, lasting at least 20 min with no apparent reduction in inhibition (Fig. 7B). These results suggest that HSNs

are inhibited in high CO₂ environments and provide a neural correlate of the striking inhibition we report at the behavioral level, consistent with HSNs' critical role in egg-laying.

AWC Responses to CO₂ Modulate HSN Activity. Do CO₂ responses in AWC inhibit HSN activity? To address this question, we first examined HSN Ca²⁺ responses to CO₂ in *tax-4* mutants. Removing *tax-4* disrupted CO₂ inhibition of HSN activity (Fig. 7 A, C, and D). Rescuing *tax-4* expression selectively in AWC, using a *pceh-36::tax-4* cDNA transgene, restored CO₂-induced inhibition of HSN to *tax-4* animals (Fig. 7 C and D). Together, our data suggest that elevated CO₂ elicits sustained cGMP-dependent increases in AWC Ca²⁺ levels that tonically depress HSN activity, inhibiting egg-laying while CO₂ remains high.

Because AWC-dependent olfactory responses involve the AIA interneurons (32), we asked if AIA is required for *C. elegans* to inhibit egg-laying at high CO₂. AIA-ablated animals robustly suppressed egg-laying at 5% CO₂, suggesting that this neuron is not essential for this behavior (Fig. S6E).

Discussion

C. elegans has an unexpected richness of CO₂-responsive cells. In addition to the previously identified BAG, AFD, and ASE neurons, the AWC olfactory neurons, the ASJ and ASK gustatory neurons, the ASH and ADL nociceptive neurons, and the amphid and phasmid glial sheath cells all respond to CO₂. AWC and ASJ may be intrinsically CO₂ sensitive: These neurons lack anatomically defined gap junctions (42), and their CO₂ responses are retained in mutants with defects in both synaptic and dense core vesicle release. Odor and CO₂-responses in AWC both involve cGMP signaling. However, although AWC is activated by the removal of attractive odors (59), it is a rise in CO₂ that activates AWC.

Our search for CO₂-sensing neurons was not exhaustive, and there is no reason to assume that CO₂ responsiveness is restricted to the neurons we have identified. Recent developments in imaging methods may facilitate a more complete description of the functional circuitry underlying the detection of CO₂ (60, 61).

CO₂ Inhibition of Egg-Laying. The choice of oviposition site is an ecologically important decision with a direct impact on species fitness. Other than having a clear preference for laying eggs on food and avoiding laying eggs in high osmolarity and in the presence of vibrational stimuli (55), how *C. elegans* choose oviposition sites is unknown (54). We show that *C. elegans* strongly and persistently inhibits egg-laying in 5% CO₂, even when food is present. The AWC olfactory neurons contribute to this inhibition, but other neurons are involved also. Previous work has shown that ablating the AWC and ASK neurons partially disrupts the stimulatory effect of food on egg-laying (62). Ca²⁺ imaging suggests that food-associated cues inhibit the AWC and ASK neurons (47). Perhaps the CO₂-evoked Ca²⁺ increases we observed in these same neurons antagonize the effects of food on ASK and AWC neurons, thereby inhibiting egg-laying.

The effects of CO₂ on egg-laying involve the HSNs, which are thought to be the executive neurons driving egg-laying events (55, 63). High CO₂ persistently inhibits HSN activity. HSNs exhibit spontaneous activity that does not require extrinsic neuronal input events (55). CO₂ inhibits this intrinsic activity, partly as a result of AWC signaling. CO₂ has been shown to regulate oviposition in several insect species, although the mechanisms involved are not understood (1).

A Large Network of Multimodal Neurons Responds to CO₂. Each of the CO₂-responsive neurons we have identified mediates responses to other sensory cues in addition to CO₂. Multimodal sensory neurons may be the norm rather than the exception in *C. elegans*. Nevertheless, the number of sensory neurons re-

sponsive to CO₂ is unusual and suggests that worms can integrate the detection of CO₂ and other cues at the earliest stages of sensory processing. Analogously, olfactory neurons in mice that respond to CO₂ are also exquisitely sensitive to the peptide hormones uroguanylin and guanylin, natural urine stimuli, as well as the volatile semiochemical carbon disulfide (64, 65). These sensors are different from the olfactory sensors initially identified in the fly that respond only (or primarily) to CO₂ stimuli (66), and this finding suggests that both worms and mice can couple the detection of CO₂ to that of other sensory cues within multimodal neurons, perhaps as an efficient strategy to glean information from a generic cue such as CO₂ (67).

Glial Cell Responses to CO₂. Amphids and phasmids are the main chemosensory organs of nematodes. Amphids contain the ciliated sensory endings of 12 chemosensory and thermosensory head neurons; phasmids contain endings of two ciliated sensory neurons. Amphid and phasmid sheath cells envelope a significant part of the sensory endings of these neurons but lack synaptic connections or gap junctions with them (www.wormatlas.org/hermaphrodite/neuronalsupport/Neurosupportframeset.html). Whether the large and persistent changes in Ca²⁺ evoked in the glial cells by CO₂ are intrinsically generated or reflect neuronal input, e.g., by volume transmission, is unclear. Moreover, it is tempting to speculate, based on their physical intimacy, that glial sheath cells could communicate with sensory neurons nonsynaptically, by ephaptic coupling, either through the exchange of ions or as a result of local electric fields (68, 69). It will be interesting to explore if the glial CO₂ responses influence neuronal CO₂ responses, or vice-versa.

Functional Significance of Complexity. What is the functional significance of having so many CO₂-responsive cells? Different CO₂-responsive neurons have different response characteristics: They can be transient or persistent and ON or OFF. Different neurons also appear to make different contributions to CO₂-evoked behaviors, depending on the exact behavior(s) studied, the experimental paradigm used, and previous experience (5). *C. elegans* thrive on rotting plant material and in microbe-rich habitats (70) where CO₂ concentrations likely vary substantially. Rather than having a single sensory channel that links the perception of CO₂ to a hard-wired behavioral response, the availability and context-dependent use of multiple sensors could allow greater behavioral flexibility. As in *C. elegans*, a variety of CO₂-responsive neurons have been identified in the mouse brain (3). Part of this complexity reflects different neurons controlling different CO₂-evoked responses, e.g., control of breathing rate or of animal arousal. Part may have evolved to enable very small changes in CO₂/H⁺ to alter the breathing rate adaptively in a highly reliable way.

In flies, CO₂ sensing initially was thought to depend on a dedicated olfactory circuit that mediates detection and innate avoidance of CO₂ (66), consistent with a labeled line-coding logic. Later work showed that avoidance of higher CO₂ concentration requires an additional, functionally segregated population of olfactory receptor neurons that likely detect CO₂-induced acidosis (71). However, flies also can exhibit behavioral attraction to CO₂ mediated by the gustatory system (72), suggesting different behaviors can be generated in different contexts by using different modes of sensory detection. The emerging pattern is that a plethora of sensory structures and cells are sensitive to CO₂, endowing animals with greater behavioral flexibility and the capacity to integrate information from multiple sources.

A future challenge is to identify the sensor molecules mediating the CO₂ responses we have described. Doing so will distinguish unambiguously between intrinsically CO₂-sensitive neurons and their downstream targets. In vertebrates the majority of CO₂-sensitive structures appear to detect changes in pH rather

than molecular CO₂ or bicarbonate (but see refs. 19 and 73). The sensory molecules implicated in these responses are diverse and include PKD2L1 and TRPA1 channels mediating gustatory and noxious responses to CO₂ (74) and acid-sensing ion channels (ASIC1A) expressed in the amygdala and bed nucleus of the stria terminalis to elicit CO₂-evoked fear responses in mice (14, 75). In addition, a variety of receptor molecules have been proposed to underlie CO₂ chemosensitivity in peripheral and central chemoreceptors essential for the control of respiration (76–78). Some of these molecules are expressed in the nervous system of the worm, including members of the TRP channel superfamily, ASICs, and inward rectifier (Kir) potassium channels (79). They may have similar roles in CO₂ sensing in *C. elegans*. At a circuitry level, we need to understand how the members of the remarkably extensive network of CO₂ responsive neurons cooperate or compete to drive behavioral responses. From an evolutionary perspective, such a network may facilitate behavioral diversification during speciation.

Methods

Strains. Strains were grown at 22 °C under standard conditions with *Escherichia coli* OP50 (80). A full strain list is provided in *SI Strain List*.

Behavioral Assays.

Locomotory responses. Assays were performed essentially as described previously (5). Briefly, 20–25 adult hermaphrodites were picked to NGM plates seeded 16–20 h earlier with 20 μL of *E. coli* OP50 grown in 2× TY medium (per litre, 16 g tryptone, 10 g yeast extract, 5 g NaCl, pH 7.4). To create a behavioral arena with a defined atmosphere, we placed a 1 cm × 1 cm × 200 μm deep polydimethylsiloxane chamber on top of the worms, with inlets connected to a PHD 2000 Infusion syringe pump (Harvard apparatus), and delivered humidified gas mixtures of defined composition at a flow rate of 3.0 mL/min. We recorded movies using FlyCapture on a Leica M165FC dissecting microscope with a Point Gray Grasshopper camera running at two frames/s. Movies were analyzed using custom-written Matlab software to detect omega turns and reversals and to calculate instantaneous speed.

Egg-laying assays. L4-stage animals were picked onto plentiful food and grown under standard conditions for 36–38 h. Individual worms then were transferred to a square-shaped bacterial lawn seeded the night before with 40 μL of *E. coli* OP50 grown in 2× TY. Assay plates were placed into a gas-tight chamber containing 5% CO₂, and controls were placed next to the chamber and otherwise treated identically. For each genotype and condition we assayed six to eight animals on each of at least three different days. After

2 h, worms were removed from the assay plate, and the number of eggs laid by each animal was counted. We used Prism 6 (GraphPad) for statistical analysis and to plot data.

For rescue experiments, nontransgenic siblings were used as controls in all experiments.

Ca²⁺ Imaging. Ca²⁺ imaging of immobilized animals was performed as described previously (5, 81) using an inverted microscope (Axiovert; Zeiss), a 40× C-Apochromat lens, and MetaMorph acquisition software (Molecular Devices). Worms were glued to agarose pads (2% in M9 buffer, 1 mM CaCl₂) using Dermabond tissue adhesive with the nose and tail immersed in a mix of OP50 and M9 buffer. Recordings were carried out at two frames/s with an exposure time of 100 ms in all experiments. Photobleaching was minimized using optical density filter 2.0 or 1.5. An excitation filter (Chroma) restricted illumination to the cyan channel, and a beam splitter (Optical Insights) was used to separate the cyan and yellow emission light. A custom-written Matlab script was used to analyze image stacks and obtain statistics.

Molecular Biology and Generation of Transgenic Lines. Expression constructs were made using the MultiSite Gateway Three-Fragment Vector Construct Kit (Life Technologies). Promoters used in this study include *sra-9* (3 kb; ASK), *sre-1* (4 kb; ADL), *trx-1* (1 kb; ASJ), *ceh-36* (334 bp; AWC), *ops-1* (1.98 kb; ASG), *flp-21* and *ncs-1* (RMG), *gcy-28d* (2.98 kb; AIA), *fig-1* (2.2 kb; glia), *sra-6* (3 kb; ASH), *odr-1* (AWC), *sra-13* (AWC), and *cat-1* (HSN). The *ceh-36* delta promoter was a kind gift from P. Sengupta, Brandeis University, Waltham, MA. The HSN imaging line driving expression of YC3.60 under a *cat-1* promoter was a gift from Robyn Branicky and Bill Schafer, MRC Laboratory of Molecular Biology, Cambridge, United Kingdom. Promoter fragments were amplified from genomic DNA and cloned into the first position of the Gateway system, genes of interest into the second position, and the *unc-54* 3' UTR or the SL2::mCherry sequence into the third position. To generate a Ca²⁺-insensitive version of the cameleon YC3.60 sensor (31), we mutated its three Ca²⁺-binding sites, replacing GAG with CAA in each case (E32Q, E68Q, and E141Q). The gene was synthesized from oligonucleotides (GeneArt; Life Technologies) and cloned into the second position of the Gateway system. Rescue and imaging constructs were injected at 30–55 ng/μL, together with a coinjection marker (*unc-122::RFP* or *unc-122::GFP*) at 50–60 ng/μL.

ACKNOWLEDGMENTS. We thank Robyn Branicky, Marios Chatzigeorgiou, Changchun Chen, Dennis Kim, Josh Meisel, Birgitta Olofsson, Niels Ringstad, Piali Sengupta, Bill Schafer, Manuel Zimmer, and the *Caenorhabditis* Genetics Center (which is funded by NIH Office of Research Infrastructure Programs P40 OD010440) for strains and/or constructs and Zoltan Soltesz, Marios Chatzigeorgiou, and Robyn Branicky for invaluable advice and critical reading of the manuscript.

- Guerenstein PG, Hildebrand JG (2008) Roles and effects of environmental carbon dioxide in insect life. *Annu Rev Entomol* 53:161–178.
- Cummins EP, Selfridge AC, Sporn PH, Sznajder JI, Taylor CT (2014) Carbon dioxide-sensing in organisms and its implications for human disease. *Cell Mol Life Sci* 71(5): 831–845.
- Huckstepp RT, Dale N (2011) Redefining the components of central CO₂ chemosensitivity—towards a better understanding of mechanism. *J Physiol* 589(Pt 23): 5561–5579.
- Stange G, Stowe S (1999) Carbon-dioxide sensing structures in terrestrial arthropods. *Microsc Res Tech* 47(6):416–427.
- Bretscher AJ, et al. (2011) Temperature, oxygen, and salt-sensing neurons in *C. elegans* are carbon dioxide sensors that control avoidance behavior. *Neuron* 69(6): 1099–1113.
- Halleme EA, et al. (2011) Receptor-type guanylate cyclase is required for carbon dioxide sensation by *Caenorhabditis elegans*. *Proc Natl Acad Sci USA* 108(1):254–259.
- Ludwig MG, et al. (2003) Proton-sensing G-protein-coupled receptors. *Nature* 425(6953):93–98.
- Wellner-Kienitz MC, Shams H, Scheid P (1998) Contribution of Ca²⁺-activated K⁺ channels to central chemosensitivity in cultivated neurons of fetal rat medulla. *J Neurophysiol* 79(6):2885–2894.
- Hibino H, et al. (2010) Inwardly rectifying potassium channels: Their structure, function, and physiological roles. *Physiol Rev* 90(1):291–366.
- Duprat F, et al. (1997) TASK, a human background K⁺ channel to sense external pH variations near physiological pH. *EMBO J* 16(17):5464–5471.
- Huang AL, et al. (2006) The cells and logic for mammalian sour taste detection. *Nature* 442(7105):934–938.
- Tominaga M, et al. (1998) The cloned capsaicin receptor integrates multiple pain-producing stimuli. *Neuron* 21(3):531–543.
- Waldmann R, Champigny G, Bassilana F, Heurteaux C, Lazdunski M (1997) A proton-gated cation channel involved in acid-sensing. *Nature* 386(6621):173–177.
- Ziemann AE, et al. (2009) The amygdala is a chemosensor that detects carbon dioxide and acidosis to elicit fear behavior. *Cell* 139(5):1012–1021.
- Preisig PA (2007) The acid-activated signaling pathway: Starting with Pyk2 and ending with increased NHE3 activity. *Kidney Int* 72(11):1324–1329.
- Chen Y, et al. (2000) Soluble adenylyl cyclase as an evolutionarily conserved bicarbonate sensor. *Science* 289(5479):625–628.
- Sun L, et al. (2009) Guanylyl cyclase-D in the olfactory CO₂ neurons is activated by bicarbonate. *Proc Natl Acad Sci USA* 106(6):2041–2046.
- Smith ES, Martinez-Velazquez L, Ringstad N (2013) A chemoreceptor that detects molecular carbon dioxide. *J Biol Chem* 288(52):37071–37081.
- Meigh L, et al. (2013) CO₂ directly modulates connexin 26 by formation of carbamate bridges between subunits. *eLife* 2:e01213.
- Putnam RW, Filosa JA, Ritucci NA (2004) Cellular mechanisms involved in CO₂ and acid signaling in chemosensitive neurons. *Am J Physiol Cell Physiol* 287(6): C1493–C1526.
- Brown D, Wagner CA (2012) Molecular mechanisms of acid-base sensing by the kidney. *J Am Soc Nephrol* 23(5):774–780.
- Levin LR, Buck J (2015) Physiological roles of acid-base sensors. *Annu Rev Physiol* 77: 347–362.
- Bretscher AJ, Busch KE, de Bono M (2008) A carbon dioxide avoidance behavior is integrated with responses to ambient oxygen and food in *Caenorhabditis elegans*. *Proc Natl Acad Sci USA* 105(23):8044–8049.
- Halleme EA, Sternberg PW (2008) Acute carbon dioxide avoidance in *Caenorhabditis elegans*. *Proc Natl Acad Sci USA* 105(23):8038–8043.
- Sharabi K, et al. (2009) Elevated CO₂ levels affect development, motility, and fertility and extend life span in *Caenorhabditis elegans*. *Proc Natl Acad Sci USA* 106(10): 4024–4029.
- Kodama-Namba E, et al. (2013) Cross-modulation of homeostatic responses to temperature, oxygen and carbon dioxide in *C. elegans*. *PLoS Genet* 9(12):e1004011.
- Carrillo MA, Guillermin ML, Rengarajan S, Okubo RP, Halleme EA (2013) O₂-sensing neurons control CO₂ response in *C. elegans*. *J Neurosci* 33(23):9675–9683.
- Zimmer M, et al. (2009) Neurons detect increases and decreases in oxygen levels using distinct guanylate cyclases. *Neuron* 61(6):865–879.

29. Ringstad N, Horvitz HR (2008) FMRFamide neuropeptides and acetylcholine synergistically inhibit egg-laying by *C. elegans*. *Nat Neurosci* 11(10):1168–1176.
30. Mank M, Griesbeck O (2008) Genetically encoded calcium indicators. *Chem Rev* 108(5):1550–1564.
31. Nagai T, Yamada S, Tominaga T, Ichikawa M, Miyawaki A (2004) Expanded dynamic range of fluorescent indicators for Ca(2+) by circularly permuted yellow fluorescent proteins. *Proc Natl Acad Sci USA* 101(29):10554–10559.
32. Chalasani SH, et al. (2010) Neuropeptide feedback modifies odor-evoked dynamics in *Caenorhabditis elegans* olfactory neurons. *Nat Neurosci* 13(5):615–621.
33. Shinkai Y, et al. (2011) Behavioral choice between conflicting alternatives is regulated by a receptor guanylyl cyclase, GCY-28, and a receptor tyrosine kinase, SCD-2, in AIA interneurons of *Caenorhabditis elegans*. *J Neurosci* 31(8):3007–3015.
34. Oda S, Tomioka M, Iino Y (2011) Neuronal plasticity regulated by the insulin-like signaling pathway underlies salt chemotaxis learning in *Caenorhabditis elegans*. *J Neurophysiol* 106(1):301–308.
35. Mulkey DK, Wenker IC (2011) Astrocyte chemoreceptors: Mechanisms of H+ sensing by astrocytes in the retrotrapezoid nucleus and their possible contribution to respiratory drive. *Exp Physiol* 96(4):400–406.
36. Gourine AV, et al. (2010) Astrocytes control breathing through pH-dependent release of ATP. *Science* 329(5991):571–575.
37. Ward S, Thomson N, White JG, Brenner S (1975) Electron microscopical reconstruction of the anterior sensory anatomy of the nematode *Caenorhabditis elegans*. *J Comp Neurol* 160(3):313–337.
38. Doroquez DB, Berciu C, Anderson JR, Sengupta P, Nicastro D (2014) A high-resolution morphological and ultrastructural map of anterior sensory cilia and glia in *Caenorhabditis elegans*. *eLife* 3:e01948.
39. Wang Y, et al. (2008) A glial DEG/ENAC channel functions with neuronal channel DEG-1 to mediate specific sensory functions in *C. elegans*. *EMBO J* 27(18):2388–2399.
40. Leinwand SG, Chalasani SH (2013) Neuropeptide signaling remodels chemosensory circuit composition in *Caenorhabditis elegans*. *Nat Neurosci* 16(10):1461–1467.
41. Suzuki H, et al. (2008) Functional asymmetry in *Caenorhabditis elegans* taste neurons and its computational role in chemotaxis. *Nature* 454(7200):114–117.
42. White JG, Southgate E, Thomson JN, Brenner S (1986) The structure of the nervous system of the nematode *Caenorhabditis elegans*. *Philos Trans R Soc Lond B Biol Sci* 314(1165):1–340.
43. Richmond JE, Davis WS, Jorgensen EM (1999) UNC-13 is required for synaptic vesicle fusion in *C. elegans*. *Nat Neurosci* 2(11):959–964.
44. Speese S, et al. (2007) UNC-31 (CAPS) is required for dense-core vesicle but not synaptic vesicle exocytosis in *Caenorhabditis elegans*. *J Neurosci* 27(23):6150–6162.
45. Macosko EZ, et al. (2009) A hub-and-spoke circuit drives pheromone attraction and social behaviour in *C. elegans*. *Nature* 458(7242):1171–1175.
46. Liu J, et al. (2010) *C. elegans* phototransduction requires a G protein-dependent cGMP pathway and a taste receptor homolog. *Nat Neurosci* 13(6):715–722.
47. Wakabayashi T, et al. (2009) In vivo calcium imaging of OFF-responding ASK chemosensory neurons in *C. elegans*. *Biochim Biophys Acta* 1790(8):765–769.
48. Coburn CM, Bargmann CI (1996) A putative cyclic nucleotide-gated channel is required for sensory development and function in *C. elegans*. *Neuron* 17(4):695–706.
49. Komatsu H, Mori I, Rhee JS, Akaike N, Ohshima Y (1996) Mutations in a cyclic nucleotide-gated channel lead to abnormal thermosensation and chemosensation in *C. elegans*. *Neuron* 17(4):707–718.
50. Kim K, Kim R, Sengupta P (2010) The HMX/NKX homeodomain protein MLS-2 specifies the identity of the AWC sensory neuron type via regulation of the *ceh-36* Otx gene in *C. elegans*. *Development* 137(6):963–974.
51. Guais A, et al. (2011) Toxicity of carbon dioxide: A review. *Chem Res Toxicol* 24(12):2061–2070.
52. Coates JC, de Bono M (2002) Antagonistic pathways in neurons exposed to body fluid regulate social feeding in *Caenorhabditis elegans*. *Nature* 419(6910):925–929.
53. Battu G, Hoier EF, Hajnal A (2003) The *C. elegans* G-protein-coupled receptor SRA-13 inhibits RAS/MAPK signalling during olfaction and vulval development. *Development* 130(12):2567–2577.
54. Schafer WR (2005) Egg-laying. *WormBook* 1–7. Available at www.wormbook.org/chapters/www_egglaying/egglaying.html. Accessed January 6, 2015.
55. Zhang M, et al. (2008) A self-regulating feed-forward circuit controlling *C. elegans* egg-laying behavior. *Curr Biol* 18(19):1445–1455.
56. Branicky R, Miyazaki H, Strange K, Schafer WR (2014) The voltage-gated anion channels encoded by *clh-3* regulate egg laying in *C. elegans* by modulating motor neuron excitability. *J Neurosci* 34(3):764–775.
57. Emtage L, et al. (2012) IRK-1 potassium channels mediate peptidergic inhibition of *Caenorhabditis elegans* serotonin neurons via a G(o) signaling pathway. *J Neurosci* 32(46):16285–16295.
58. Leifer AM, Fang-Yen C, Gershow M, Alkema MJ, Samuel AD (2011) Optogenetic manipulation of neural activity in freely moving *Caenorhabditis elegans*. *Nat Methods* 8(2):147–152.
59. Chalasani SH, et al. (2007) Dissecting a circuit for olfactory behaviour in *Caenorhabditis elegans*. *Nature* 450(7166):63–70.
60. Prevedel R, et al. (2014) Simultaneous whole-animal 3D imaging of neuronal activity using light-field microscopy. *Nat Methods* 11(7):727–730.
61. Schrödel T, Prevedel R, Aumayr K, Zimmer M, Vaziri A (2013) Brain-wide 3D imaging of neuronal activity in *Caenorhabditis elegans* with sculpted light. *Nat Methods* 10(10):1013–1020.
62. Sawin ER (1996) Genetic and cellular analysis of modulated behaviors in *Caenorhabditis elegans*. Biology Ph.D. Thesis, (MIT, Cambridge, MA).
63. Zhang M, Schafer WR, Breitling R (2010) A circuit model of the temporal pattern generator of *Caenorhabditis elegans* egg-laying behavior. *BMC Syst Biol* 4:81.
64. Leinders-Zufall T, et al. (2007) Contribution of the receptor guanylyl cyclase GC-D to chemosensory function in the olfactory epithelium. *Proc Natl Acad Sci USA* 104(36):14507–14512.
65. Munger SD, et al. (2010) An olfactory subsystem that detects carbon disulfide and mediates food-related social learning. *Curr Biol* 20(16):1438–1444.
66. Suh GS, et al. (2004) A single population of olfactory sensory neurons mediates an innate avoidance behaviour in *Drosophila*. *Nature* 431(7010):854–859.
67. Scott K (2011) Out of thin air: Sensory detection of oxygen and carbon dioxide. *Neuron* 69(2):194–202.
68. Jefferys JG (1995) Nonsynaptic modulation of neuronal activity in the brain: Electric currents and extracellular ions. *Physiol Rev* 75(4):689–723.
69. Su CY, Menzies K, Reiser J, Carlson JR (2012) Non-synaptic inhibition between grouped neurons in an olfactory circuit. *Nature* 492(7427):66–71.
70. Félix MA, Braendle C (2010) The natural history of *Caenorhabditis elegans*. *Curr Biol* 20(22):R965–R969.
71. Ai M, et al. (2010) Acid sensing by the *Drosophila* olfactory system. *Nature* 468(7324):691–695.
72. Fischler W, Kong P, Marella S, Scott K (2007) The detection of carbonation by the *Drosophila* gustatory system. *Nature* 448(7157):1054–1057.
73. Hu J, et al. (2007) Detection of near-atmospheric concentrations of CO₂ by an olfactory subsystem in the mouse. *Science* 317(5840):953–957.
74. Chandrashekar J, et al. (2009) The taste of carbonation. *Science* 326(5951):443–445.
75. Taugher RJ, et al. (2014) The bed nucleus of the stria terminalis is critical for anxiety-related behavior evoked by CO₂ and acidosis. *J Neurosci* 34(31):10247–10255.
76. Wang W, Bradley SR, Richerson GB (2002) Quantification of the response of rat medullary raphe neurons to independent changes in pH(o) and P(CO₂). *J Physiol* 540(Pt 3):951–970.
77. Lahiri S, Forster RE, 2nd (2003) CO₂/H(+) sensing: Peripheral and central chemoreception. *Int J Biochem Cell Biol* 35(10):1413–1435.
78. Jiang C, Rojas A, Wang R, Wang X (2005) CO₂ central chemosensitivity: Why are there so many sensing molecules? *Respir Physiol Neurobiol* 145(2-3):115–126.
79. Hobert O (2013) The neuronal genome of *Caenorhabditis elegans*. *WormBook*, ed. The *C. elegans* Research Community (WormBook.org). Available at www.wormbook.org/chapters/www_neuronalgenome/neuronalgenome.pdf. Accessed June 2, 2015.
80. Sulston J, Hodgkin J (1988) *The Nematode Caenorhabditis elegans*, ed Wood WB (Cold Spring Harbor Lab Press, Cold Spring Harbor, NY), pp 587–606.
81. Busch KE, et al. (2012) Tonic signaling from O₂ sensors sets neural circuit activity and behavioral state. *Nat Neurosci* 15(4):581–591.